Adv Syst Sci Appl 2018; **02**; 26-52
Published online at http://ijassa.ipu.ru/index.php/ijassa/article/view/598

Plasma Control in Tokamaks. Part 1. Controlled Thermonuclear Fusion Problem. Tokamaks. Components of Control Systems.

Yuri Mitrishkin[1,2*], Pavel Korenev[1,2], Artem Prokhorov[1,2], Nikolay Kartsev[2], Mikhail Patrov[3]

[1)] *M. V. Lomonosov Moscow State University, Faculty of Physics, Moscow, Russia*

[2)] *V. A. Trapeznikov Institute of Control Sciences, Russian Academy of Sciences, Moscow, Russia*

[3)] *Ioffe Institute, Russian Academy of Sciences, St. Petersburg, Russia*

Abstract: Various concepts of tokamaks as leaders in solving the controlled thermonuclear fusion problem are presented. The evolution of tokamaks from round in vertical cross-section tokamaks with a large aspect ratio up to tokamaks with a small aspect ratio including spherical ones is characterized. The classification of modern tokamaks according to their poloidal systems with the location of the poloidal field coils inside and outside of the toroidal field coil is given, taking into account the presence of coils inside a vacuum vessel to stabilize the plasma position. The methods of plasma diagnostics by magnetic measurements outside the plasma, actuators for both plasma magnetic and kinetic control, associated with plasma additional heating, plasma magnetic and kinetic models, instabilities and disruptions of a plasma discharge are described.

Keywords: controlled thermonuclear fusion, thermonuclear power station, tokamak, plasma, tokamak classification, diagnostics, additional plasma heating, actuators, plasma equilibrium reconstruction, plasma magnetic and kinetic models, plasma instabilities, disruptions, spherical tokamaks.

1. INTRODUCTION

The aim of the survey is to present a plasma in a tokamak as a complex unstable time-varying multivariable nonlinear plant with distributed parameters and uncertainties to be controlled and to explore magnetic and kinetic plasma control systems and their development trends.

The plasma in a tokamak [1–4] has toroidal axial-symmetric magnetic configuration which is superposition of fields created by the currents in toroidal field coils, plasma distributed current, and currents in poloidal field coils. An abbreviation “tokamak” (from Russian *toroidal chamber with magnetic coils*) was proposed in the I.V. Kurchatov Institute of Atomic Energy (Moscow, Russia). A variable magnetic field produced by the current in a central solenoid (inductor) induces a vortex electrical field, which breaks down gas, typically hydrogen, in a vacuum vessel and creates plasma, which is fully ionized gas with distributed current. Thus, tokamak is a current transformer.

A plasma column tends to gain its major radius because of the integral plasma current at axial-symmetric points is oppositely directed which leads to self-pushing. Additionally, the major radius is gained by the gas kinetic pressure in plasma. Hence, a feedback control system is needed to stabilize a horizontal plasma position by a vertical magnetic field.

The plasma in modern tokamaks is vertically elongated that allows to increase plasma pressure for the same toroidal field. Unfortunately, it leads to plasma vertical instability. Hence,

* Corresponding author: yvm@mail.ru

a feedback control system is necessary to stabilize an unstable plasma vertical position by a horizontal magnetic field.

A multivariable plasma shape control system is needed to keep a high-temperature plasma near the tokamak first wall. The plasma current can be controlled either by a controller in a separate loop or by the multivariable controller for plasma shape and current simultaneously [5–7].

While plasma pressure increases unstable resistive wall modes (RWM) may also occur. Hence, additional actuating coils and feedback control system are needed to suppress RWM [8].

Based on the facts listed above one can conclude that modern tokamak devices must be developed in parallel with plasma magnetic control systems.

Neutral atom injection and electromagnetic waves are used for additional plasma heating, which provides ability to plasma kinetic control, i.e. control of plasma current profile [9, 10], stability margin [11], pressure, and temperature [12] in order to optimize plasma discharge parameters. Magnetic and kinetic control integration [13] will be the basis for reliable plasma control systems of future thermonuclear reactors.

The survey consists of four parts. Different construction concepts of modern tokamaks and different magnetic and kinetic plasma control systems, which are used in real experiments or in numerical simulations of present tokamaks are considered.

Part 1 is devoted to the general problem of the controllable thermonuclear synthesis, main distinctive tokamak features, and plasma control systems. Construction and diagnostics system of the spherical Globus-M tokamak (Ioffe Institute, St. Petersburg, Russia) are described. Results of Globus-M experiments were used in Lomonosov MSU and Trapeznikov ICS to develop original plasma position, current, and shape control systems.

Plasma magnetic control systems are presented in parts 2 and 3. Part 4 is dedicated to plasma kinetic control systems and their integration with magnetic control systems to achieve optimal tokamak operation regimes in stationary and transition modes to get maximum stability margins and acceptable performance.

2. CONTROLLED THERMONUCLEAR FUSION

At present, the primary source of energy for the humankind is burning organic fossil fuels namely coal, oil, and gas. Although natural reserves of fossil fuels will not be completely exhausted for several hundred years, experts predict an energy deficit in less than 50 years at current consumption rates [14]. Renewable energy sources such as solar energy, hydroelectric power, geothermal energy, and wind energy are attractive from an environmental point of view, but cannot provide sufficient energy output to become a full-fledged substitute for the fossil fuels. Nuclear power stations, which harness energy released in the fission reactions of atoms of heavy elements, can produce sufficient amounts of energy, but, unfortunately, the by-products of fission are very radioactive and long-lived. Additionally, nuclear power plants require careful monitoring of all operational parameters, since an accidental release of radioactive substances would have the disastrous impact on the environment and could exceed the impact from thermoelectric power stations.

One of the most promising sources of the future energy is thermonuclear fusion reactions, which are merging of the nuclei of the light elements like hydrogen, for example. Although the controlled thermonuclear fusion is an extremely complex technological problem, the thermonuclear power has significant advantages over existing energy sources. In particular, fuel reserves for thermonuclear reactions on the Earth will last for many thousands of years, since the necessary hydrogen isotopes can be obtained from water and widely available lithium. Hydrogen nuclear fusion reactions do not lead to air pollution or formation of greenhouse gases, since the product of the fusion reaction is helium. In contrast with nuclear fission, nuclear fusion does not involve uncontrolled chain reactions, which means that there

is no risk of a nuclear accident. The point is that at any time one can close the valves of fuel feeding into the tokamak vacuum vessel and by this action to stop the fusion process. We also note that a thermonuclear reactor does not produce long-lived radioactive waste. The main radioactive by-products of the reactor are neutron-activated materials (i.e., materials which become radioactive because of a neutron bombardment of the first wall of tokamaks), which can be minimized by material selection for the reactor vessel. Most of the radioactive materials produced in the reactor can be safely and easily disposed of after use and utilized harmless in several decades, unlike most fission by-products that require special storage and processing for thousands of years.

There are many possible reactions of nuclear fusion, which differ by the required conditions and the amount of energy released. However, the most promising is the fusion reaction of hydrogen isotopes: deuterium and tritium

$$ {}^{2}_{1}\mathrm{D} + {}^{3}_{1}\mathrm{T} \rightarrow {}^{4}_{2}\alpha + {}^{1}_{0}\mathrm{n} + 17.6\,\mathrm{MeV}. \tag{2.1} $$

When the nuclei of deuterium and tritium fuse, an alpha-particle and a neutron are formed. The alpha-particles may remain in the plasma and contribute energy to maintain the thermonuclear reaction. The neutrons carry 80% of the released energy and are absorbed by reactor's first wall, transforming energy into heat, which can be converted into electricity. The deuterium-tritium fuel has an extremely high density of energy: 1 g. of the mixture is equivalent to 10 000 liters of oil! A small portion of the energy generated by the reactor can be used to extract deuterium from seawater, while tritium can be produced by neutron bombardment of lithium.

Since the nuclei of atoms are positively charged, according to Coulomb's law they repel each other. At ordinary temperatures, no fusion reactions occur, since the atoms do not have enough energy to overcome the Coulomb barrier. The temperature required for the thermonuclear reaction is about 10^9 K. At these temperatures, the fuel is in the state of completely ionized gas such as plasma. For a positive energy output, the plasma in the reactor must satisfy the Lawson criterion [2] $n\tau T > 3\cdot 10^{21}\ \mathrm{m}^{-3}\ s\times\mathrm{keV}$, where τ is the energy confinement time, during which the plasma retains enough energy for the reaction to occur, n is the plasma particle density, and T is the plasma temperature.

3. TOKAMAKS

3.1. Tokamaks evolution

The first tokamak was constructed in 1954 in the Kurchatov Institute of Atomic Energy, and after that the researches of plasma confinement in tokamaks began in many laboratories in the world. Since 1954 221 tokamaks have been built and 41 of them are working nowadays [15].

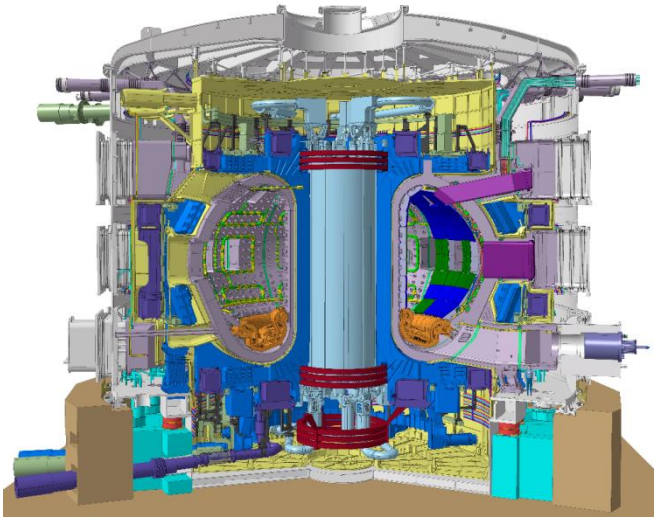

Fig. 3.1. View of ITER.[1]

The evolution of tokamaks began from devices with a circular cross section which were surrounded by a copper shell and led to modern vertically elongated ones [2]. In the first tokamaks the plasma speed was damped by induced Foucault currents in the tokamak copper shell that was acting as the controller of a direct action. In modern devices, the magnetic and kinetic active feedback control systems are used. Magnetic plasma control systems [2, 6, 7, 16] evolved from simple scalar plasma horizontal position control systems to multivariable plasma position, current, and shape control systems. For the last 30 years, power generated by tokamaks increased in 108 times [14]. Such a significant progress was achieved due to the qualitative jump in the development of the plasma physics and in the level of understanding of processes occurring during plasma discharges.

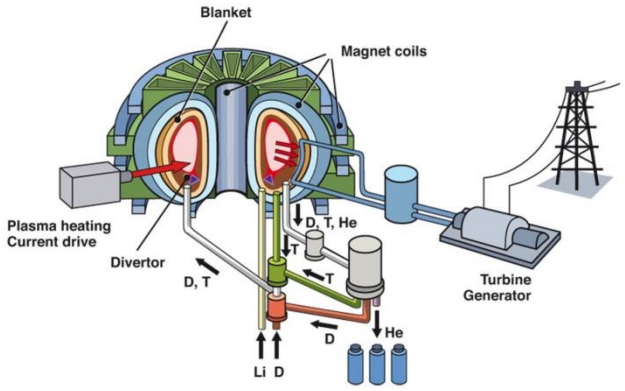

Fig. 3.2. Deuterium-tritium thermonuclear power plant scheme.[2]

The fundamental task, which arises when developing modern tokamaks, is the search of the methods and approaches to provide optimal and reliable thermonuclear fusion. Most of researches of plasma confinement and heating on operating tokamaks are directed to support the ITER project (International Thermonuclear Experimental Reactor) [17] (Fig. 3.1), which has to open the way to the DEMO project (DEMOnstration Power Plant). The DEMO is the first future noncommercial thermonuclear power plant (Fig. 3.2) [18]. The ITER tokamak will be the first thermonuclear experimental reactor, which will produce ten times more energy than consumes. The international community with participants from European Union, Japan, USA, Russia, China, South Korea, and India is developing and constructing the ITER.

Table 3.1 shows comparative characteristics of the ITER tokamak-reactor and the thermonuclear power plant DEMO [18] based on the tokamak principle. DEMO will be the last step before the construction of commercial thermonuclear power plants. In contrast to

[1] ITER Organization, http://www.iter.org/.
[2] Max-Planck-Institute-fur-Plasmaphysik: http://www.ipp.mpg.de/986351/fusion_e.pdf.

ITER, which is the experimental device for high temperature plasma researches, DEMO will be more close to future industrial reactors, more technological for the aims of reliable exploitation and replacement of components. It will have optimized cooling system for higher temperatures at energy generation, less diagnostics, and minimal set of subsystems, which is necessary for working. The time of plasma discharge in DEMO will be more than two hours with self-sustained thermonuclear fusion reaction. The results obtained on ITER will permit to narrow the range of requirements down and at the same time to optimize them on DEMO.

Table 3.1. Characteristics of the ITER experimental reactor and the thermonuclear power plant DEMO [18]

Parameter	ITER $A = 3.1$	DEMO 1 $A = 3.1$	DEMO 2 $A = 2.6$
Aspect ratio $A = R/a$	6.2/2.0	9.1/2.9	7.5/2.9
Elongation k / triangular δ	1.7/0.33	1.6/0.33	1.8/0.33
Surface area, m^2 / Plasma volume, m^3	683/831	1428/2502	1253/2217
Plasma current, MA	17	20	22
Major radius toroidal field, T	5.3	5.7	5.6
Discharge time, sec	400	> 7200	> 7200
Output thermonuclear power, MW / generated power, MW	500/0	2037/500	3255/953
R and a are major and minor radiuses, k and δ are elongation and triangularity (see Fig. 5.2).			

3.2. Principles of tokamak operation

The electromagnetic fields produced by a current-carrying coils in a tokamak effect on plasma charged particles and are used for plasma confinement and control in the limited vessel volume. The poloidal and toroidal magnetic fields generated by currents in poloidal and toroidal coils and the magnetic field generated by the plasma current compose the resulting helical magnetic field (Fig. 3.3). Plasma charged particles cannot leave such a magnetic configuration while moving on Larmor radii along helical magnetic lines with cyclotron frequencies inside the torus. The toroidal field of tokamaks usually a tenfold greater than the poloidal field and is around several units of tesla. The toroidal field coil has a large number of turns and a current about several kA traveling through the coil creates the same field as a current about several MA traveling through one turn. Depending on the resistance of the coil (usually copper or superconducting), the voltage from several units to hundred units is needed for steady state mode, but for transition processes the requirements are significantly higher. There are tokamaks, for example JET (UK), with an iron core inside the central solenoid to increase magnetic flux inducting plasma current. However, most of the tokamaks do not have iron cores, for example DIII-D (USA).

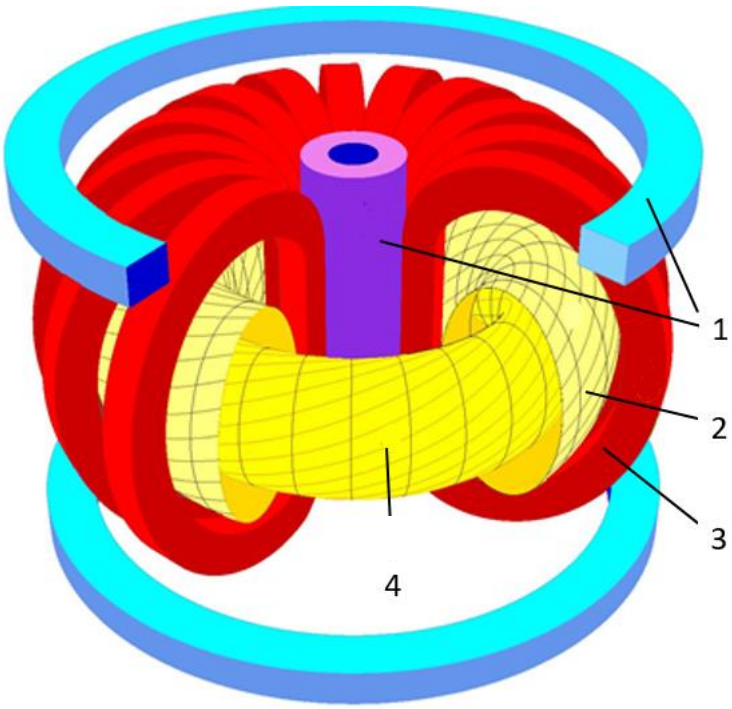

Fig. 3.3. Vertically elongated tokamak without an iron core: 1 is the poloidal field inner and outer coils; 2 is the vacuum vessel; 3 is the toroidal field coil; 4 is plasma and helical magnetic lines.[3]

Tokamak magnetic fields make outer pressure, which balances plasma inner kinetic pressure. Thus, a small magnetic field disturbance can lead to a local expansion of the plasma, which will exponentially grow if not suppressed. Magnetohydrodynamic (MHD) theory [19] can describe most of such plasma instabilities.

The varying field of the central solenoid induces the electrical field, which creates the plasma current analogously to a field produced by the current in the primary transformer winding induces a current in the secondary winding. However, the solenoid current must continuously grow to maintain the plasma current, this fact constrains the plasma discharge time. That is why other non-ohmic current sources are needed. The most promising are a bootstrap current inducing by a plasma charged particles density gradient, and an additional heating current.

3.3. Modern tokamaks poloidal system classification

Table 3.2 shows the main characteristics of the present vertically elongated tokamaks with the most advanced plasma control systems (see survey parts 2–4 in the next journal issues), the ITER experimental reactor under construction, and the DEMO project for the thermonuclear power plant.

Table 3.2. Characteristics of present tokamaks, ITER, and DEMO

Device	Country	Starting year	Major radius, m	Minor radius, m	Toroidal field, T	Plasma current, MA
DIII-D [20]	USA	1986	1.66	0.67	2.2	3.0
NSTX [21]	USA	1999	1.85	0.65	0.3	1.4
JT-60U [22]	Japan	1991	3.40	1.00	2.7	5.5
TCV [23]	Switzerland	1992	0.88	0.25–0.7	1.4	1.2
JET [24]	UK	1992	3.00	1.25–2.1	4.0	6.0

[3] Project Center ITER (Russia): http://www.iterrf.ru/upload/docs/Booklet_new.pdf.

ASDEX Upgrade [25]	Germany	1991	1.65	0.5–0.8	3.9	1.4
EAST [26]	China	2006	1.75	0.4–0.8	5.0	0.5
KSTAR [27]	South Korea	2008	1.8	0.5	3.5	2.0
ITER [28, 29]	France	2025	6.2	2.0	5.3	17
DEMO 1 [18]	–	2040–2045	9.1	2.9	5.7	20.0

The poloidal systems of present vertically elongated tokamaks may be differentiated on three main groups.

- «Warm» poloidal field coils are inside the toroidal coil, the plasma vertical position control coil is outside the vacuum vessel. Such tokamaks are NSTX, DIII-D (USA), JT-60U (Japan), TCV (Switzerland).
- «Warm» poloidal field coils are outside the toroidal coil, the plasma vertical position control coil is outside the vacuum vessel. Such tokamaks are JET (UK), ASDEX Upgrade (Germany), Globus-M (Russia).
- Superconducting poloidal field coils are outside the toroidal coil, the plasma vertical position control coil is inside the vacuum vessel. Such tokamaks are EAST (China), ITER (France), KSTAR (South Korea). In tokamaks KSTAR [27] and JT-60SA [30] the plasma vertical position control coil and the plasma horizontal position control coil are inside the vacuum vessel, which considerably enhances the efficiency of control.

3.4. Plasma auxiliary heating in the tokamaks

When the Lawson criterion [2] is satisfied, the plasma generates enough heat to maintain its temperature, but to achieve that, Joule heating by plasma current is not enough, there is a need for *auxiliary* plasma heating. Auxiliary heating of the plasma can also be used to control the profiles of its current, temperature, and pressure in order to achieve energetically favorable operating conditions and suppress MHD instabilities.

The plasma current I_p generates Joule heat $P \sim \eta I_p^2$ where η is the plasma resistivity. However, with increasing the plasma temperature the resistivity of the plasma decreases according to the law $\eta \sim T^{-3/2}$, therefore ohmic heating ceases to be effective at high temperatures and auxiliary heating methods are needed.

One of the main methods of auxiliary heating is neutral beam injection heating. The electromagnetic field does not prevent the entry of neutral particles into the plasma, where they transfer their kinetic energy to plasma in collisions with its particles. For example, deuterium beams with a power of 20 MW are used in tokamaks DIII-D [20] and ASDEX Upgrade [25].

Another method of the plasma heating is based on the use of radio waves that resonate with plasma particles and transmit their energy to them. There are heating by the radio waves with the ion cyclotron frequency (tens of megahertz) and with an electron cyclotron frequency (hundreds of gigahertz). For example, on the DIII-D tokamak, ion cyclotron heating (30-120 MHz, 6 MW) and electron cyclotron heating (110 GHz, 6 MW) are used [31], the ASDEX Upgrade tokamak includes the ion (30-120 GHz, 6 MW) and electron (140 GHz, 4 MW) cyclotron heating [32, 33]. The TCV tokamak uses the electron cyclotron heating system, consisting of 9 gyrotrons (82 and 118 GHz, 4.5 MW) [12, 23]. The EAST tokamak uses ion cyclotron heating (27 MHz, 6 MW) [34].

4. PLASMA MAGNETIC DIAGNOSTICS

Measuring systems are the most important components of the plasma control systems of any tokamak. They allow to determine the physical quantities describing the behavior and structure of the heated plasma inside the tokamak vessel and to perform plasma diagnostics. Measuring devices that require physical contact with plasma even for a short time period are extremely limited, since a high-temperature plasma can quickly disable them. Infrared sensors are also used in experiments, but they do not provide measurements with sufficient time resolution for the most purposes of plasma control [35]. The simplest and most widely used method to detect the boundary and integral parameters of the plasma is the use of magnetic sensors measuring the changes in the magnetic field and flux outside the plasma [4, 6, 35], but within the region of the magnetic field produced by the plasma.

All sensors related to magnetic diagnostics work on the same basic principle, namely: the induced electromotive force U_0 in any coil is equal to the time rate of change of the magnetic flux passing through this coil, taken with a minus sign (in accordance with the Faraday's law):

$$U_0 = -N\frac{d\Phi}{dt} = -N\frac{d}{dt}\int \vec{B}d\vec{S}, \tag{4.1}$$

where N is the number of coil turns, Φ is the magnetic flux passing through the coil, $\vec{B}$ is the magnetic induction field.

To describe electromagnetic phenomena in tokamaks, the function of the poloidal flux $\psi(\vec{r},t) = \frac{1}{2\pi}\int\limits_{S(\vec{r})} \vec{B}d\vec{S}$ as a magnetic flux per one radian passing through a circle S centered on the vertical axis of the tokamak is usually introduced (Fig. 4.1). This function depends on the coordinate $\vec{r}$ on the poloidal plane and on the time t.

The magnetic flux sensor consists of a single turn of wire, also called a loop. The flux loop is usually located outside the vacuum vessel in the toroidal direction. The poloidal magnetic flux in a tokamak is measured by integrating the voltage U_0, which is proportional to the electromotive force induced in the flux loop (Fig. 4.1). The integrated loop voltage with a corresponding coefficient is a poloidal magnetic flux passing through its circuit:

$$\psi(\vec{r},\, t) = -\frac{1}{2\pi}\int_{t_0}^{t} U_0(\tau)d\tau + \psi(\vec{r},\, t_0). \tag{4.2}$$

For axisymmetric plasma, this measurement gives the value of the poloidal flux at a certain point of the poloidal plane.

The saddle loops are constructed by connecting two sectors of poloidal loops measuring poloidal fluxes at points $\vec{r}_1$ and $\vec{r}_2$. Their integrated voltage is proportional to the difference between poloidal fluxes:

$$\psi(\vec{r}_1,\, t) \;-\; \psi(\vec{r}_2,\, t) = -\frac{1}{2\pi}\int_{t_0}^{t} U_0(\tau)d\tau + \psi(\vec{r}_1,\, t_0) \;-\; \psi(\vec{r}_2,\, t_0). \tag{4.3}$$

The magnetic field is measured using the magnetic probes (Fig. 4.1), which react to the change in the magnetic flux passing through them. A magnetic probe is a multi-turn coil connected to a voltage sensor. Assuming that there is the homogeneity of the magnetic field inside the coil, the induced voltage U_0 is related to the local magnetic field by the relation

$$\vec{B}(\vec{r},\, t)\vec{n} = -\frac{1}{NS}\int_{t_0}^{t} U_0(\tau)d\tau + \vec{B}(\vec{r},\, t_0)\vec{n}, \tag{4.4}$$

where $\vec{n}$ is the normal vector to a cross section of the coil, N is the number of turns, S is the cross-sectional area of the coil. This expression is approximate since the magnetic flux is not constant at the edges of the probe.

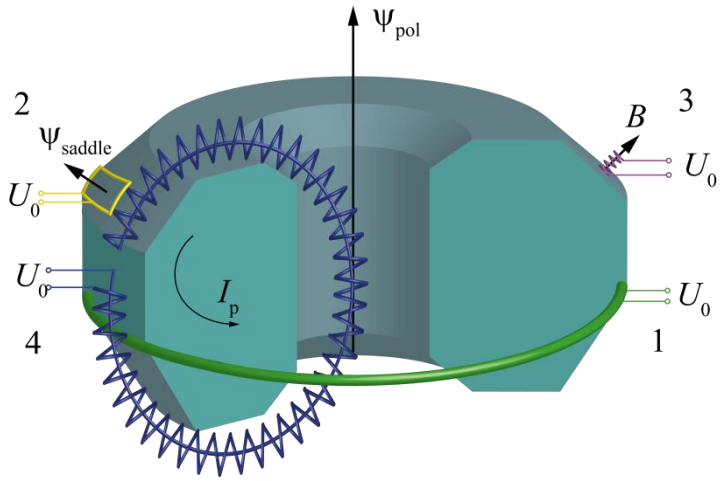

Fig. 4.1. Magnetic measurements in tokamak: 1 is the magnetic loop; 2 is the saddle loop; 3 is the magnetic probe; 4 is the Rogowski coil.

In order to measure the plasma current in tokamaks, Rogowski coils are used. Fig. 4.1 shows Rogowski loop, which measures the sum I_{sum} of the plasma toroidal current I_p and the current in the vacuum vessel that passes through the region bounded by the coil, based on integrating the magnetic field in a closed loop around the measured current. According to Ampere's circuital law, the electric current passing through the loop is determined through the integrated magnetic field around this closed loop $I = \frac{1}{\mu_0}\oint \vec{B}d\vec{l}$, where μ_0 is the vacuum permeability. If individual turns of the Rogowski loop are small in comparison with the overall size of the coil, then the magnetic field $\vec{B}$ remains almost unchanged along this turn and the flux measured per unit length of coil is given by $d\Phi = nS\vec{B}\,d\vec{l}$, where n is the number of turns per unit length of the coil, S is the cross-sectional area of the coil. Then the total magnetic flux penetrating Rogowski's loop is equal to the value $\Phi = nS\oint \vec{B}\,d\vec{l}$ and the measured plasma current is determined by the equation:

$$I_{sum}(t) = \frac{\Phi(t)}{\mu_0 nS} = -\frac{1}{\mu_0 nS}\int_{t_0}^{t} U_0(\tau)d\tau + I_{sum}(t_0). \qquad (4.5)$$

The magnetic diagnostics is the main function of the measuring complex of any tokamak. Consideration of other types of diagnosis goes beyond the scope of this review. We note only their great diversity, which arises, first of all, because of the features of the high-temperature plasma emitting in a wide spectrum of wavelengths: from the range of visible wavelengths to the hard X-rays, and also because of the need to control not only the integral parameters of the plasma, but also local values of physical quantities inside the plasma.

5. PLASMA MODELS

5.1. Plasma evolution modelling

The MHD plasma equilibrium in a tokamak is usually described by the poloidal flux function ψ proportional at the point P to the magnetic induction flux through the circle S perpendicular to the Z axis and passing through the point P (Fig. 5.1). Knowing the poloidal flux distribution, the plasma boundary can be found as the largest *closed* constant level line of the poloidal flux inside the tokamak vessel, and in accordance with the Gauss theorem $\mathrm{div}\,\vec{B} = 0$ the poloidal magnetic field is expressed as $\vec{B}_p = \nabla\psi \times \nabla\varphi$.

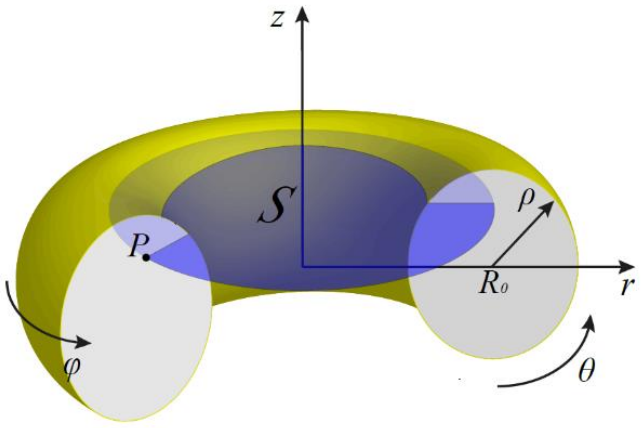

Fig. 5.1. Cylindrical r, φ, z and toroidal coordinates ρ, φ, θ in a tokamak

From the Ampere's law $\mathrm{curl}\,\vec{B} = \mu_0 \vec{J}$, where $\vec{J}$ is the plasma current density vector, μ_0 is the vacuum permeability, the force balance equation $\vec{J} \times \vec{B} = \nabla p$ and the axial symmetry of the tokamak the Grad-Shafranov equation describing the plasma equilibrium is derived [2, 4, 6]. In cylindrical coordinates it has a form:

$$r \frac{\partial}{\partial r} \frac{1}{r} \frac{\partial \psi}{\partial r} + \frac{\partial^2 \psi}{\partial z^2} = -\mu_0 r^2 \frac{dp}{d\psi} - F \frac{dF}{d\psi}, \tag{5.1}$$

where p is the plasma pressure, and function $F(\psi)$ is related to the magnetic toroidal field as $F(\psi) \equiv rB_\varphi$.

In the limit of the infinite plasma conductivity, the contour lines of the poloidal flux are "frozen" into the plasma, and the value of the poloidal flow on the plasma boundary does not change. However, the plasma resistance is not small enough to be neglected during the tokamak discharge, and the MHD equilibrium of the plasma undergoes evolution in accordance with Ohm's law. The projection of the Ohm's differential law onto magnetic lines in the plasma is called the magnetic diffusion equation. In the limit of the large aspect ratio and the circular cross section of the plasma, it has the form [36]:

$$\sigma_{\|} \frac{\partial \psi}{\partial t} = \frac{1}{\mu_0 \rho} \frac{\partial}{\partial \rho} \rho \frac{\partial \psi}{\partial \rho} + r J_{ni}, \tag{5.2}$$

where $\sigma_{\|}$ is the conductivity of the plasma along the magnetic lines, and J_{ni} is the density of non-ohmic currents, including bootstrap current and currents created by the auxiliary heating systems.

In order to calculate conductivity and non-ohmical currents for the magnetic diffusion equation, pressure and density profiles of the electrons and plasma ions are needed. They are found by solving the transport equations for plasma particles and energy in the plasma [37]:

$$\begin{aligned} \frac{\partial n_\alpha}{\partial t} + \nabla \left(n \vec{u}_\alpha \right) &= S_\alpha, \\ \frac{3}{2} \frac{\partial p_\alpha}{\partial t} + \nabla \left(\vec{q}_\alpha + \frac{5}{2} p_\alpha \vec{u}_\alpha \right) &= P_\alpha, \end{aligned} \tag{5.3}$$

where the index $\alpha = i, e$ indicates the type of particles (ions or electrons), n_α is the particle density, S_α is the particle sources, $\vec{q}_\alpha$ is the heat flux, $\vec{u}_\alpha$ is the particles velocity, P_α is the power of the energy sources, including ohmic and auxiliary heating, including the energy exchange between electrons and ions, as well as the radiation losses. These quantities are taken from theoretical or (since there is currently no complete theory of transport processes in a tokamak) from empirical models, depending on the mode of tokamak operation.

5.2. Nonlinear plasma evolution codes

5.2.1. Free boundary codes

To solve the plasma evolution equations, a number of plasma-physical codes have been developed. They consist of two groups. The first group contains codes that model plasma with a free boundary. For example, the non-linear dynamic plasmophysical tokamak plasma model was developed in the State Reserch Center of RF "Troitsk institute for innovation & fusion research (TRINITI)" (Troitsk). The model is based on a two-dimensional equilibrium of a plasma with a free boundary in the external magnetic field, the transport and magnetic diffusion equations, averaged over magnetic surfaces, and a system of active coils of the poloidal field, and a passive stabilization structure. The model is numerically implemented in the DINA code [37].

In different countries and for different tokamaks, other nonlinear codes with a free plasma boundary were created, differing from the DINA code by various features (a nonzero plasma mass, different numerical methods, etc.): TSC (Tokamak Simulation Code, USA) [38], JETTO (Italy) [39], CORSICA (USA) [40], UEDGE (USA) [41], PET (Russia) [42], SCoPE (Russia) [4], EDGE2D (England) [43], MAXFEA (Italy) [44], B2-IRENE (Germany) [45], PARASOL (Japan) [46], and others.

5.2.2. Fixed boundary codes

The second group contains codes that model plasma with a fixed boundary specified by the user. These include many codes created to model the transport processes in the plasma. They are ASTRA (Russia) [47], CRONOS (France) [48], TRANSP and PTRANSP [49, 50], ONETWO [51], and BALDUR [52] (all USA).

Transport codes can be used in conjunction with free boundary plasma codes, forming a hybrid transport-magnetic model. For example, the DINA-CH code has been combined with the CRONOS code [53], and the TSC code [38] has been combined with the code PTRANSP [50].

5.3. Linearization of nonlinear plasma models

To solve the problems of controlling the plasma shape, current, and position in a tokamak it is generally required to keep the plasma near the desired equilibrium position. The smallness of the deviations from the equilibrium, which is provided by feedback control systems, allows to describe the plasma by linear models. There are different approaches to designing control systems for linear models. The basic equation for these problems is the nonlinear differential Kirchhoff's equation describing the interconnected magnetic system of conductors with currents, including the plasma [54, 55]:

$$\dot{\Psi} + RI_c = Nu, \;\; N = \begin{bmatrix} \Xi_{m\times m} \\ 0_{(n-m)\times m} \end{bmatrix}, \;\; \Psi, I_c \in R^n, u \in R^m, n > m, \tag{5.4}$$

where Ψ is the vector of poloidal fluxes averaged over the cross sections of the conducting elements and penetrating them in vertical planes, I_c is the vector of currents in the active poloidal field coils and in the passive elements, R is the impedance matrix of the conducting elements, u is the vector of external voltages applied to the active poloidal field coils, u is *the input* of the controlled plant, $\Xi_{m\times m}$ is the unit matrix of the size $m\times m$, $0_{(n-m)\times m}$ is the zero matrix of the size $(n-m)\times m$. Nonzero values in the matrix N correspond to the voltages applied to the active poloidal field coils, while the zero values correspond to zero voltages applied to the passive elements.

The linearized Kirchhoff's equation for small deviations from the equilibrium position has the form:

$$\frac{\partial \Psi}{\partial I_c}\delta \dot{I}_c + \frac{\partial \Psi}{\partial I_p}\delta \dot{I}_p + \frac{\partial \Psi}{\partial \vec{r}_p}\delta \dot{\vec{r}}_p + \frac{\partial \Psi}{\partial \xi}\delta \dot{\xi} + R\delta I_c = N\delta u. \tag{5.5}$$

Where I_p is the total plasma current, $\vec{r}_p$ is the vector of plasma magnetic axis coordinates, ξ is the vector of parameters describing the current profile such as the ratio of the gas kinetic pressure to the pressure of the poloidal magnetic field β_p and the internal plasma inductance l_i: $\xi = \begin{bmatrix} \beta_p & l_i \end{bmatrix}^T$. The form of the poloidal plasma cross section is conveniently described as follows:

$$h = h\left(I_c,\, I_p,\, \vec{r}_p,\, \xi\right), \tag{5.6}$$

where I_c is the vector of currents in the active poloidal field coils and in the passive elements, I_p is the total plasma current, $\vec{r}_p$ is the position of the magnetic axis and ξ is the perturbation vector. Using the linearization of this equation, we obtain:

$$y = \delta h = \frac{\partial h}{\partial I_c}\delta I_c + \frac{\partial h}{\partial I_p}\delta I_p + \frac{\partial h}{\partial \vec{r}_p}\delta \vec{r}_p + \frac{\partial h}{\partial \xi}\delta \xi. \tag{5.7}$$

Deviation of the plasma current δI_p can be described by the linearized Kirchhoff's equation for the plasma or expressed in terms of deviations δI and $\delta\xi$ taking into account the physical condition that magnetic field line freezing-in into the plasma: $\bar{\Psi} = \frac{1}{I_p}\int_S J\Psi dS = \text{const}$, where J is the plasma current density and hence:

$$\frac{\partial \bar{\Psi}}{\partial I_c}\delta I_c + \frac{\partial \bar{\Psi}}{\partial I_p}\delta I_p + \frac{\partial \bar{\Psi}}{\partial \vec{r}_p}\delta \vec{r}_p + \frac{\partial \bar{\Psi}}{\partial \xi}\delta \xi = 0. \tag{5.8}$$

Similarly, the displacement of the plasma position $\delta\vec{r}_p$ can be described by the motion equation $m\ddot{\vec{r}}_p = \vec{F}$, or, neglecting the mass of the plasma, is linearly expressed based on the forces $\vec{F}$ acting on the plasma balance equation:

$$\frac{\partial \vec{F}}{\partial \vec{r}_p}\delta \vec{r}_p + \frac{\partial \vec{F}}{\partial I_c}\delta I_c + \frac{\partial \vec{F}}{\partial I_p}\delta I_p + \frac{\partial \vec{F}}{\partial \xi}\delta \xi = 0. \tag{5.9}$$

The resulting system of equations of the linear plasma model in the state space representation has the form:

$$\begin{aligned} \delta \dot{I} &= A\delta I + B\delta u + E\delta \dot{\xi}, \\ y &= C\delta I + F\delta \xi, \end{aligned} \tag{5.10}$$

where A, B, C, E and F are Jacobi matrices. The state vector δI includes current deviations in the active and passive tokamak elements and it could also include the deviation of the total plasma current δI_p, the displacement of the plasma position $\delta\vec{r}_p$ and its velocity $\delta\dot{\vec{r}}_p$. If we exclude the derivative $\delta\dot{\xi}$ from the first equation of the given system by changing the variables $x \equiv \delta I - E\delta\xi$, then the equations of the linear model, taking into account the notation $u = \delta u$, take the standard form of the linear dynamical system representation. Since the vector of the external perturbation is presented in both equations, it allows simulating "the minor disruptions" in the plasma of tokamaks:

$$\begin{aligned} \dot{x} &= Ax + Bu + AE\delta \xi, \\ y &= Cx + (CE + F)\delta \xi. \end{aligned} \tag{5.11}$$

We emphasize that in the model there is no static connection between the control vector u and the output vector y in terms of the ABCD representation of the linear dynamical system: the matrix D is zero. Through the matrices AE and CE + F, the perturbation $\delta\xi$ turns into the

state and output equations of the plant model. The control action u is included only into the state differential equation and is not included in the output equation. Physically, it is explained by the fact that the current in the plasma and its magnetic configuration cannot change instantaneously under the influence of control signals, since it takes some time for the electromotive force to penetrate into the plasma, all this creates the dynamics of the propagation of the control action into the plasma. Mathematically, the description of this process reduces to solving a two-dimensional partial differential equation for the voltage being induced in plasma [4].

5.4. Plasma equilibrium reconstruction

Plasma evolution codes can calculate distributions of the current density and poloidal flux for any point of time during the modelled discharge. However, in the experiments these distributions are unknown, so plasma shape and the profiles of plasma parameters are to be identified from the signals of the tokamak diagnostic system. This inverse problem is called the *plasma equilibrium reconstruction* problem [35].

The plasma equilibrium reconstruction problem is to find the distribution of the poloidal flux ψ, the plasma region S and the plasma toroidal current density distribution J in it, satisfying the Grad-Shafranov equation:

$$r\frac{\partial}{\partial r}\frac{1}{r}\frac{\partial \psi}{\partial r}+\frac{\partial^2 \psi}{\partial z^2}=\begin{cases}-\mu_0 rJ, & (r,z)\in S,\\ 0, & (r,z)\notin S,\end{cases}$$
$$J=rp'(\psi)+\frac{1}{\mu_0 r}F(\psi)F'(\psi) \tag{5.12}$$

with boundary conditions $\psi\big|_{r=0}=\psi\big|_{r=\infty}=0$ and consistent with the indications of the available magnetic diagnostics, which usually include the total plasma current $\int_S JdS=I_p$, measurements of the poloidal flux in the set of N points outside the plasma $\psi(\vec{r}_i)=\Psi_i,\ i=1,...,N$, and the poloidal magnetic field in the set of M points outside the plasma $\nabla\psi(\vec{r}_j)\times\nabla\varphi(\vec{r}_j)=\vec{B}_{pj},\ j=1,...,M$. Additional restrictions on the current density distribution, based on the measurements of kinetic parameters and safety factor profile q are possible.

One of the most common approaches to solving the equilibrium reconstruction problem is to use the method based on the Picard iterations with linear parametrization of the plasma current density [56-58]. In this method, at each iteration the functions p' and FF' from the Grad-Shafranov equation, are approximated as linear combinations of basis functions depending on the poloidal flux values of the previous iteration:

$$p'_n=\sum_k a_k\alpha_k(\psi_{n-1}),\ F_nF'_n=\sum_l b_l\beta_l(\psi_{n-1}). \tag{5.13}$$

Here, coefficients a_k and b_l are obtained at each iteration through minimization of the error functional, which may be, for example, quadratic functional of the errors between the calculated and measured values of the total plasma current, the poloidal flux, and the poloidal magnetic field. Since the plasma equilibrium reconstruction problem is ill-posed in the sense of Hadamard, the regularization techniques are used, for example, Tikhonov regularization or SVD truncation [59]. This procedure is repeated at each iteration until the convergence of the solution is achieved.

The described algorithm is computationally expensive, and simplifications are required for its application in real-time tokamak experiments. Possible simplification is truncation to the single iteration step and using the distributions calculated at the previous time point as initial values. Another possible modification is the representation of the plasma in the form of a set of filaments [60], which are concentric ideal conductors with currents that approximate the

plasma current distribution of the plasma. In this case, the plasma current density is approximated as a linear combination of delta functions. Filaments may be fixed in space, or may be moving, with the coordinates determined by the minimization of the error functional.

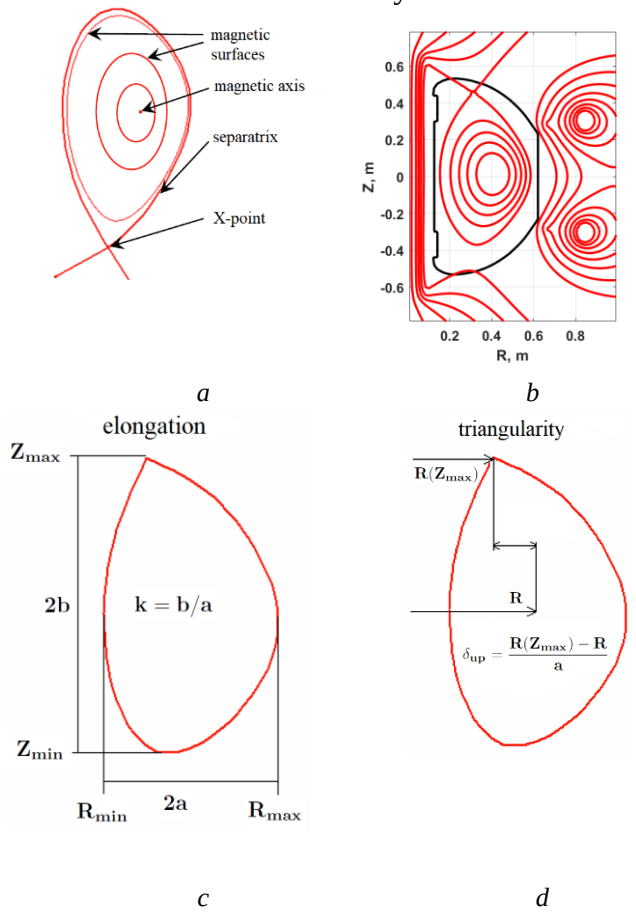

Fig. 5.2. Magnetic configurations: a – magnetic surfaces in a tokamak; b – configuration with upper X-point in Globus-M tokamak; c – definition of plasma elongation; d – definition of plasma triangularity

The filament method does not allow reconstruction of the profiles of plasma parameters, but it can be used when it is sufficient to determine the plasma position and shape. Algorithms that reconstruct the plasma shape but do not restore poloidal flux distribution are also suitable for such tasks. An example of such an algorithm is the XLOC code [61], which approximates the poloidal flux in the vacuum region by the polynomial functions satisfying $\Delta^*\psi = 0$ but does not reconstruct the poloidal flux in the plasma region. The XLOC algorithm determines plasma boundary, as a level line of the poloidal flux, containing the X-point characterized by $\nabla\psi = 0$. Another possible solution for such problems is to use algorithms based on the regression analysis of a large amount of experimental data [62].

It is mathematically rigorously shown [4] that magnetic measurements alone are insufficient to determine the internal parameters of the plasma, such as the current and pressure profiles. Being ill posed the problem of the equilibrium reconstruction, in general, may have several solutions that differ substantially in the internal plasma parameters and does not continuously depend on the input data.

The method based on the use of ε-nets and implemented in the SDSS code (*Substantially Different Solutions Searcher*, Russia) [63-67] allows to overcome these difficulties. An equilibrium reconstructed by any other method, for example, one of the above, is used as an initial approximation in this method. Then an ε-net of the right-hand sides of the Grad-Shafranov equation is constructed in a neighborhood of this equilibrium, which allows one to approximate any equilibrium in the neighborhood with an error not exceeding ε. The equilibria corresponding to the elements of the ε-net can be analyzed to find all essentially different solutions of the reconstruction problem and their errors estimations.

In Fig. 5.2, *a* magnetic surfaces (surfaces of the constant poloidal flux) in a tokamak plasma are shown, Fig. 5.2, *b* shows equilibrium of the Globus-M tokamak plasma, reconstructed with FCDI code [58]. Fig. 5.2, *c*, *d* show the geometric parameters of the plasma separatrix. The major radius of the plasma is the arithmetic mean between the maximal and the minimal radial coordinate of the separatrix $R = (R_{\max} + R_{\min})/2$, while the minor radius is their half-difference $a = (R_{\max} - R_{\min})/2$, the plasma elongation is the ratio of the vertical and radial dimensions of the plasma $k = (Z_{\max} - Z_{\min})/(R_{\max} - R_{\min})$, the upper triangularity of the plasma is the horizontal distance between the upper point of the separatrix and the major radius, divided by the minor radius $\delta_{up} = (R(Z_{\max}) - R)/a$, the lower triangularity is defined similarly $\delta_{down} = (R(Z_{\min}) - R)/a$.

6. INSTABILITIES AND DISRUPTIONS

The Grad-Shafranov equation describes the equilibrium plasma configuration in a tokamak, but it does not reflect equilibrium stability. The MHD stability studies consider evolution of the plasma equilibrium under various perturbations ξ, for example, $\xi(r)e^{i(\omega t + m\theta - n\varphi)}$ (see Fig. 5.1). Perturbations of this form are called modes and characterized by the mode numbers *m*, *n* and frequency ω. To ensure the equilibrium stability it is necessary for all possible modes to be damped or have characteristic times much longer than the discharge duration. Stability analysis is an extremely complex problem, which cannot be solved analytically in many cases. However, it is necessary to solve this problem, since plasma instabilities can lead to plasma disruptions, during which magnetic confinement is lost, and the plasma comes into contact with the walls of the tokamak, can lead to accidents and may damage the device. For example, during disruptions in the JET tokamak there were large mechanical forces acting on the wall, reaching values of several hundred kilo-newtons [2].

Since plasma disruptions cannot be allowed to occur in an operating thermonuclear reactor, research of their causes is of crucial importance. In order to learn how to suppress plasma disruptions their models are being constructed from experimental data and plasma interactions with the tokamak walls are studied [69]. In these processes the halo-currents flowing between the plasma and tokamak walls seem to play an important role [2, 69].

Plasma instabilities impose limitations on the operating parameters of the tokamak. It is because of MHD instabilities that strong magnetic fields are necessary for the tokamak operation. In order to suppress the instabilities the ratio β of the kinetic plasma pressure *p* to the magnetic field pressure $B^2/2\mu_0$ is required to have values of the order of ~ 10^{-2} or less. After analysis of the large amount of experimental data of various tokamaks an empirical limit for the value of β in stable equilibrium was calculated [70]:

$$\beta_{\max} = \left(\frac{p}{B^2/2\mu_0} \right)_{\max} = 0.028 \frac{I}{aB} \left[\frac{\text{MA}}{m \cdot T} \right], \tag{6.1}$$

where *a* is the minor plasma radius. This condition also limits the allowable plasma pressure in the tokamak.

An important parameter describing plasma stability is the safety factor *q* [2], defined for a magnetic surface *L* as $q(L) = \frac{1}{2\pi} \oint_L \frac{B_\varphi}{rB_p} dl$ where the integration is performed over the poloidal section of the surface, B_φ and B_p are toroidal and poloidal magnetic fields. In the limit of the large aspect ratio (*R*/*a*) and the circular plasma cross-section, the profile $q(\rho)$ is

expressed as $q(\rho)=\dfrac{2\pi\rho^2 B_\varphi}{\mu_0 R I(\rho)}$ where $I(\rho)$ is the plasma current profile. Thus, the restrictions on the profile q are lead to the restrictions on the current profile.

The stability analysis of the mode $m=1$ leads to the crucial *Kruskal-Shafranov stability limit* [70, 71]

$$q(a)=\frac{aB_\varphi(a)}{RB_\theta(a)}>1. \tag{6.2}$$

The limit leads to the necessity of exceeding the ratio of the toroidal $B_\varphi(a)$ and poloidal $B_\theta(a)$ components of the magnetic field over the aspect ratio *R/a*. This is equivalent to limiting the possible total plasma current for a given value of toroidal magnetic field:

$$I_p<\frac{2\pi a^2 B_\varphi}{\mu_0 R}. \tag{6.3}$$

The stability conditions can depend not only on the total plasma current, but also on the shape of the current profile. For example, a plasma with a flat profile and with an abrupt drop at the plasma edge is unstable with respect to all $m>1$ modes, therefore a small current gradient is desirable at the plasma boundary. The presence of a surface with a safety factor $q=2$ near the separatrix leads to excitation of the tearing modes associated with the finite conductivity of the plasma, which lead, in turn, to the tearing and the reconnection of the magnetic lines resulting in the formation of "magnetic islands." This phenomenon in turn enhances plasma transport processes and leads to the plasma disruption. Therefore, in practice, the safety factor restriction is strengthened to $q(a)>3$.

As the plasma is heated, its conductivity and the current density at the center of the plasma also increase, which leads to a decrease of the safety factor $q(0)$. When a value $q(0)<1$ is reached, the unstable mode m = 1 is excited, which leads to a sudden drop of the density and temperature at the center of the plasma after which the plasma heating starts again. Such temperature and density oscillations are called *sawtooth oscillations*. The physics of sawtooth oscilations is not completely understood, but it is known that the amplitude and period of the oscillations are influenced by the presence of fast ions and the plasma pressure, as well as the steepness of the q profile. Sawtooth oscillations do not lead to the plasma disruptions and are considered as part of the normal tokamak operation, but they can negatively affect the stability of other modes. For this reason, some tokamaks have sawtooth oscillations control systems, which use neutral particles injectors and radio-frequencies heating to regulate amplitude of the oscillations.

The plasma density limit is also related to the safety factor restrictions. As the density increases, the transport processes associated with the collision frequency are accelerated, which leads to the increasing of energy loss at the plasma boundary due to radiation and decreasing of the boundary layer temperature. As the temperature decreases, the resistance of the boundary layer increases, and the layer ceases to conduct current, diminishing the effective plasma volume, and reducing the safety factor q at the effective boundary, which causes subsequent plasma disruption. To maintain stability the plasma density n should not exceed the density limit established by Greenwald [72]:

$$n[10^{20}\ \mathrm{m}^{-3}]<\frac{I_p}{\pi a^2}\left[\frac{\mathrm{MA}}{\mathrm{m}^2}\right]. \tag{6.4}$$

For the problems with the fixed plasma density n this condition may be interpreted as a restriction on the minimal total plasma current I_p.

Overall MHD perturbations have a significant effect on the plasma discharges and are one of the primary causes of plasma confinement deterioration and abrupt ending of a discharge. For this reason, the search for the discharge scenarios free from the large-scale MHD

instabilities is an urgent problem in modern tokamaks. In addition to creating relatively stable magnetic configurations of a plasma column, instability suppression active methods are also employed. For example, auxiliary heating at electron cyclotron resonance frequencies can be used to control the pressure profile, preventing the development of unstable modes.

In the tokamak research, much attention is being paid to the search for plasma configurations with increased pressure, temperature, density, and energy confinement time, allowing to approach the Lawson's criterion for plasma ignition. However, such configurations are often subject to new instabilities. For example, usually on modern tokamaks the vertically elongated plasma is studied. In comparison with the circular configuration, the elongated plasma makes it possible to achieve a much higher pressure for the same magnetic field strength. To elongate the plasma vertically, a horizontal magnetic field, directed in opposite directions in upper and lower parts of the plasma is created (Fig. 6.1). However, in this configuration, small plasma displacements along the vertical are enhanced by the Ampere's forces $\vec{J} \times \vec{B}_R$, and the plasma is vertically unstable. Therefore, a feedback control system that regulates currents in horizontal field coils and stabilizes the position of the plasma is necessary for the operation of modern tokamaks.

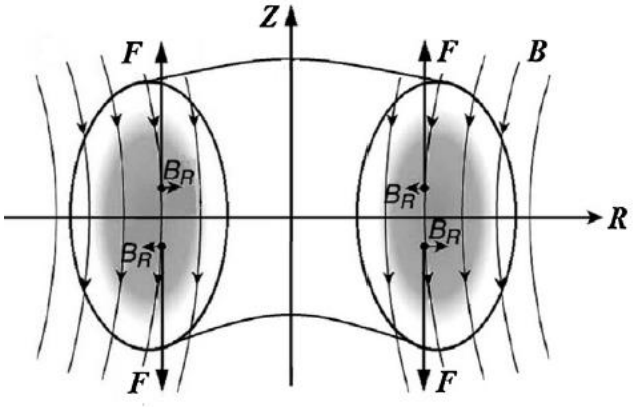

Fig. 6.1. Illustration of the vertical instability of the elongated plasma

Another promising tokamak plasma configuration is the so-called H-mode (High-confinement), which is created by intense auxiliary heating and is characterized by a significantly increased energy confinement time. However, this mode is subject to the ELM-instabilities (Edge Localized Modes). These modes, as a rule, have $n \sim 10$, $m \sim 30$, lead to periodic eruptions of plasma energy, cause confinement deterioration, and may damage the tokamak vessel. Heating of the plasma edge region and axial asymmetric magnetic fields are applied to control amplitude and frequency of the ELM outbursts.

7. ACTUATORS AND THEIR MODELS OF PLASMA MAGNETIC CONTROL SYSTEMS

The plasma magnetic sensors and diagnostics are connected via controllers to power actuators (supplies) to control plasma position, current, and shape. These actuators connected to the magnetic field coils in the feedback control system are as follows: multiphase thyristor rectifier (Fig. 7.1, *a*) [73–74], power transistor voltage inverter (Fig. 7.1, *b*) [75–77], and thyristor current inverter (Fig. 7.1, *c*) [78].

Thyristor rectifiers are relatively slow so usually they are used for the toroidal field coil supply as well as for plasma current and shape control [79, 80]. In some cases, thyristor rectifiers are applied for plasma position control together with other thyristor rectifies of poloidal field coils, for example on ASDEX Upgrade [33]. The thyristor rectifier model used for linear controller synthesis is approximated with sufficient accuracy by the transfer function of the first order with transport delay $W(s) = k e^{-Ts} / (Ts+1)$, where k is the gain and the time constant T depends on particular rectifier properties [79].

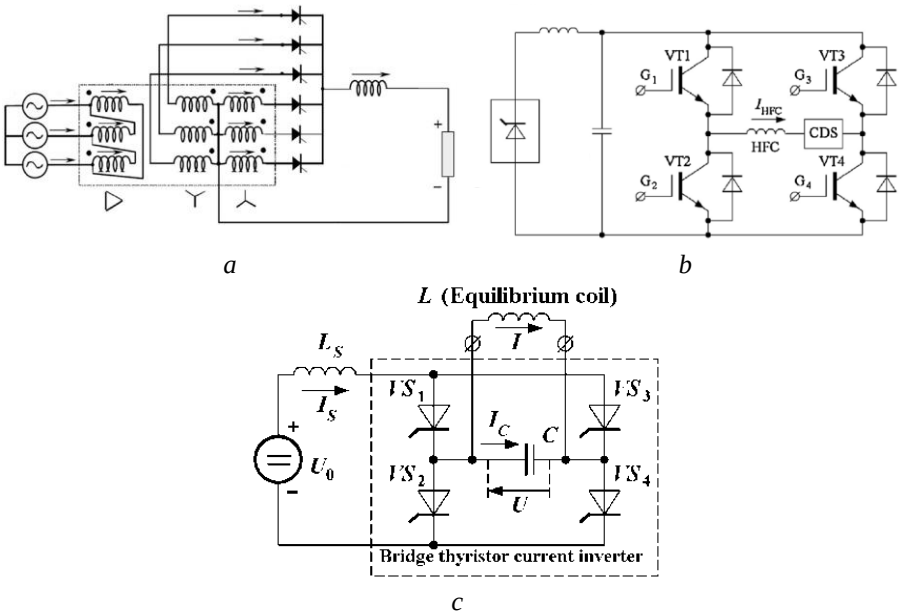

Fig. 7.1. Power parts of actuators: a – multiphase thyristor rectifier; b – transistor voltage invertor; c – thyristor current inverter

The voltage and current inverters have higher speed of response in comparison with thyristor rectifiers and are used to supply poloidal field coils or separate coils of vertical and horizon field to stabilize plasma horizon and unstable vertical position respectively [78, 80]. The models of the actuators are complex and nonlinear. However, for the controller synthesis purpose a simple gain coefficient approximation is often enough [80, 82, 83] because the actuator nonlinear dynamics is faster than the controlled processes. The voltage inverters can work in pulse-width modulation mode [76, 77] or relay mode providing sliding regime or self-oscillation processes [78, 83] in a closed-loop control system.

8. SPHERICAL TOKAMAK GLOBUS-M

8.1. Globus-M tokamak structure

The spherical tokamak (ST) Globus-M is a new generation ST that has been built for studying the physical processes in a plasma of the spherical configuration and generating engineering recommendations for STs of a MA diapason [84].

The main ST Globus-M parameters are as follows: plasma current 0.3MA, toroidal magnetic field $B_T \leq 0.4$T; major and minor radiuses are $R = 0.36$ m and $a = 0.24$ m, respectively, that correspond to the aspect ratio R/a = 1.5. The plasma elongation k upper limit is 2.2, while triangularity δ is 0.4.

The electro-magnetic tokamak system has been constructed according to the conventional scheme, when all the coils are located outside the vacuum vessel, and the poloidal magnetic field coils are kept outside the toroidal ones (Fig. 8.1).

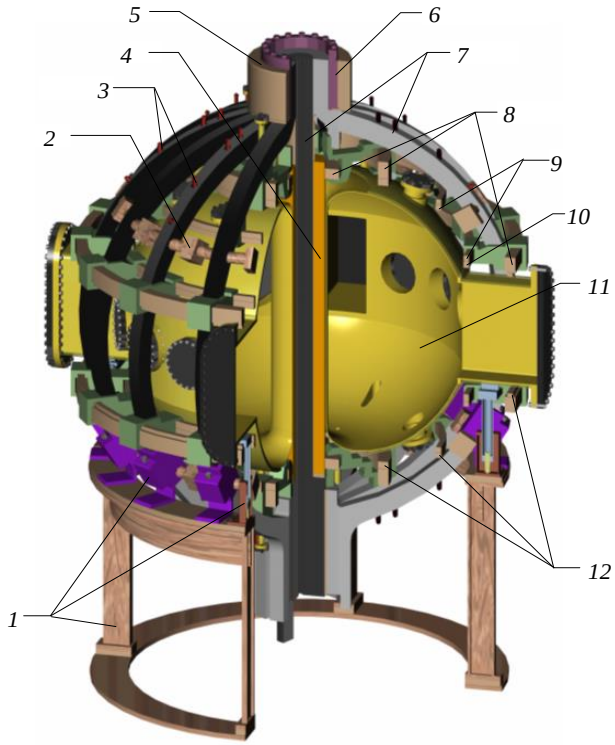

Fig. 8.1. Globus-M ST: 1 – support structure; 2 – toroidal coils separators; 3 – poloidal coils binding; 4 – central solenoid; 5 – bandage ring; 6 – wedge clamp; 7 – toroidal field coils; 8 – "slow" poloidal field coils; 9 – "fast" control coils (horizontal field); 10 – "fast" control coils (vertical field); 11 – vacuum vessel; 12 – compensation coils

Sixteen single turn D-shaped coils, constructed from the electro-technical copper, are series-connected and form the toroidal field coil. The coil parts that go through the inner cylinder of the vacuum vessel are constructed as 16 isolated bronze segments. A coil used to generate a curl electric field, i.e. a central solenoid is located at the central kernel. This solenoid is created from the copper-silver alloy and has a form of a two-layer coil for which the total height is 1.3 m. Nine pairs of the poloidal coils can be divided into three functional groups, which are scattered field compensation coils, "slow" and "fast" coils to trace the position and shape of plasma. A poloidal coil system allows to create both, single or double-nulled limiter and divertor configurations.

A small distance (around 2-3 cm) between the outer magnetic surface of the plasma column and the first wall of the vacuum vessel is very attractive. This is a key feature that differs the Globus-M ST from other STs. Application of the tokamak structure when the plasma fits the whole volume of the vacuum vessel has a range of benefits. The tokamak poloidal magnetic field coils can be set very close to the plasma itself without the necessity of putting them into the vacuum vessel. This, in turn, reduces a volume of created external magnetic field along with a reduction in a power used to create it. Moreover, the coil structure itself becomes simpler, as there are fewer requirements to provide a heat removal compared to the coils in the vacuum.

In addition, there are a number of benefits used in a diagnostic system design. For example, the magnetic sensors can be located close to the external magnetic surface of the plasma, the wider angle of view for the plasma observation may be realized via diagnostic sockets. There are some disadvantages associated with the Globus-M construction specifically a higher load on the first wall of the tokamak due to a small area of the vessel compared to the plasma volume; also, much stronger requirements to the plasma control system (small transition process time, power supply speed of response in the control contour, and accuracy).

The coils of the tokamak are fed from six-phase thyristor rectifiers and fast thyristor current inverters with frequency up to 3 kHz connected to the high-voltage AC line of 110 kV through power transformers. The power supplies are enveloped by feedback loops, which allow to

maintain plasma position, shape, and current at their references. The cooling system of the coils provides the tokamak operation at the frequency of six discharges per an hour with duration of a discharge about 0.3 s and the maximal achieved plasma current of 0.36 MA. The working plasma current range is 180–250 kA. The plasma current is maintained by the flux change of the poloidal coils with average volt-second area of 0.33 Vs. The central solenoid contribution to the average magnetic flux is 90%.

The Globus-M vacuum vessel is an all-welded stainless steel construction and has the volume of about 1.1 m^3. There are 38 diagnostic sockets having an overall area of 0.8 m^2, which provide good access to plasma for diagnostics and additional heating. The vacuum vessel is welded from an inner cylinder with a wall thickness of 2 mm, two hemispheres with a wall thickness of 3 mm and a thick outer ring with a thickness of 14 mm. The total resistance of the vessel is 120 μOhm in the toroidal direction. About 50% of the current flows through the inner cylinder, 35% through the hemispheres and only 15% through the outer ring. Such a small current through the external ring is explained by the presence of sockets. In fact, the current flows in two rings with a height of about 4 cm. The construction of the sockets allows to inject additional heating power into the plasma up to 4 MW (fundamental and high harmonics of ion-cyclotron frequency [85], injection of a neutral atom beam [86]). The main part of the plasma-facing surface, which is more exposed to plasma flows, is protected by the tiles made of a special type of graphite RG-Ti91. The details of construction of the tokamak are also described in [87].

8.2. Diagnostic systems of the Globus-M tokamak

The tokamak diagnostics complex used in the experiments consists from a large number of monitor diagnostic systems working permanently. These are current and voltage sensors in a tokamak magnetic system, the series of loops and probes for the magnetic measurements, UHF-interferometer, optic (collimated and survey sensors of luminosity lines of hydrogen and deuterium, sensors of light impurities radiation, survey spectrometers) and x-ray detectors (soft and hard radiation), bolometers, Langmuir probes, etc. [88, 89].

Depending on the experimental aims, systems that are more complicated can be connected. Some of them require an operator action; others transfer a large amount of extra data into the database of the installation. They are Thomson scattering diagnostic [90], charge exchange recombination systems, fast optical band video capturing. The scheme in Fig. 8.2 shows the location of the main diagnostic units and general tokamak systems.

Reconstruction of the plasma magnetic configuration is based on the magnetic coils measurements [91] (21 in total on Globus-M) located on the tokamak discharge vessel surface to measure the poloidal flux. The EFIT code [56] performs this reconstruction in the off-line mode. The UHF-interferometer measures the plasma density in a monitoring mode with the following settings: wavelength is 0.8 mm; vertical chords are located on 24, 42, and 50 cm from the tokamak axis. The apparatus allows reasonably measuring a linear density in a range till 0.6×10^{20} m^{-2} that corresponds to the averaged plasma density around 1.0×10^{20} m^{-3}.

Thomson scattering (TS) [90] is used to measure the plasma electron temperature and density profiles. Measurements are taken along the minor radius from the inner side of the plasma column. A total number of spatial points is 10. The TS makes it possible to achieve up to 20 measurements per discharge for the pre-defined time points. A minimal interval between the neighboring measurements is not more than 500 μs. The ion temperature is determined using the CXRS (charge exchange recombination spectroscopy) with the help of the AKORD-12 analyzer [89]. Its observation line is directed along the tokamak major radius. This analyzer can measure the neutral hydrogen and deuterium flows at the same time by 6 energetic channels for each isotope. A minimal time resolution is 1 ms. The observation line of the second similar analyzer is toroidally oriented.

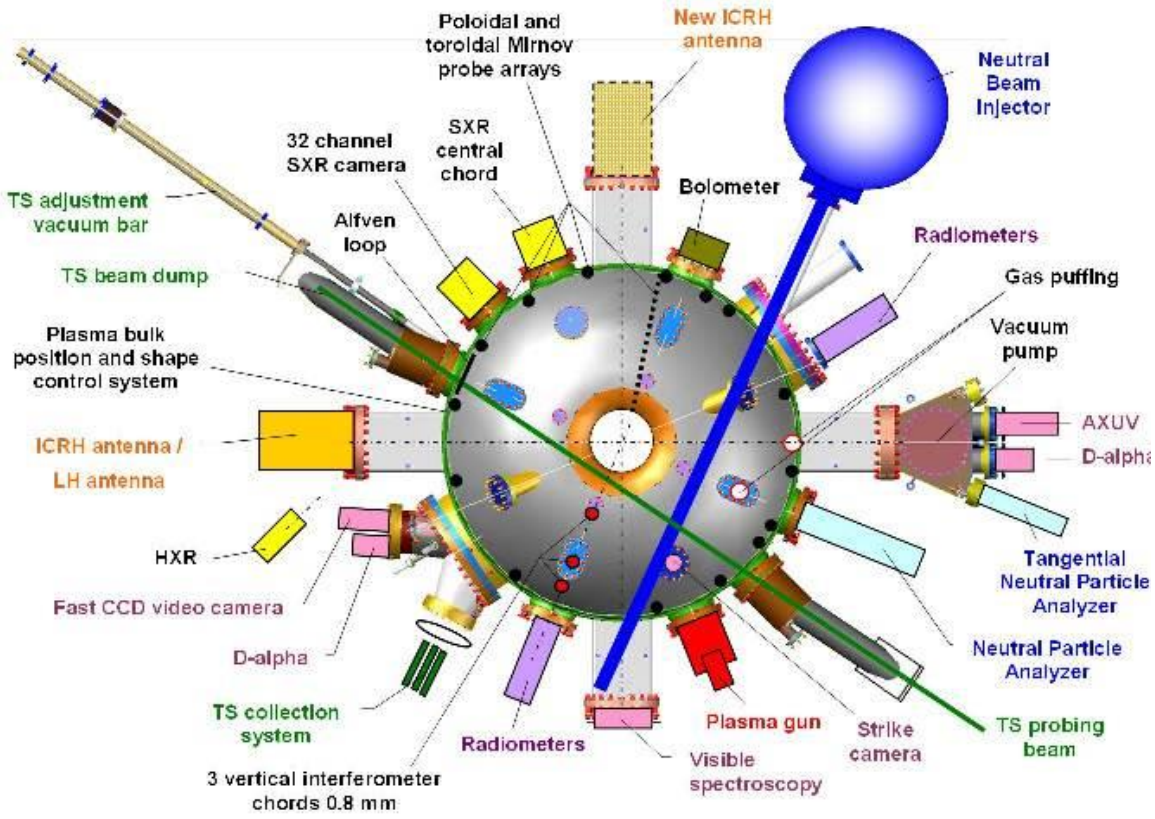

Fig. 8.2. The scheme of location of general Globus-M tokamak systems and diagnostics: view from the top; poloidal magnetic system is not showed

The key feature of the Globus-M ST in comparison with the other spherical machines is an extremely high chord-averaged density in a plasma column. It varies from 1.4 to 1.8 MA /m^2 in different operating modes. Thus, the Ohmic mode becomes more effective because of the specific heating power is proportional to the squared plasma current density. The high current density as well as a high ratio B_T/R that reaches 1.8 T/m permit obtaining discharges with high averaged plasma density limit around 10^{20} m^{-3} even in the Ohmic mode discharges.

9. CONCLUSION

The survey outlines different features of modern vertically elongated tokamaks as plants under control through examples of some present tokamaks and ITER, which is currently under construction. The report from developers of the first thermonuclear power plant DEMO [18] shows that the project is realizable and time limit of construction is determined.

Described state of the art of the ITER and DEMO projects defines the roadmap to final solution of controllable thermonuclear fusion problem in the foreseeable future.

The main differences between present tokamaks are as follows: toroidal field coil placement inside or outside the poloidal field coils, putting the plasma position control coils inside or outside the vacuum vessel, superconductivity property of magnet coils, and so on. Superconductive coils are proposed to use in the DEMO project, but its poloidal system structure is still in the phase of research.

Considered problems of the plasma diagnostics and design of tokamak actuators show an additional complexity of plasma control systems development, for synthesis and analysis of these systems linear and nonlinear plasma models presented are necessary.

Nowadays, main tokamak plasma instabilities are suppressed. The most dangerous phenomenon for future thermonuclear power plants are so called “major disruptions” [2, 69, 92] which must not occur in tokamaks-reactors. This phenomenon is being studied and the ways not to admit this effect are under research. These ways are right assignment of profiles

of plasma kinetic parameters by means of plasma kinetic control systems and their optimal interaction with the plasma magnetic control systems.

ACKNOWLEDGEMENTS

This work was supported by the Russian Science Foundation (RSF), grant No 17-19-01022 (sections 1-7) and the Russian Foundation for Basic Research (RFBR), grant No 17-08-00293 (section 8).

REFERENCES

1. Artsimovich, L. A. (1972). Tokamak devices. *Nuclear Fusion*, 12(2), 215-252, https://doi.org/10.1088/0029-5515/12/2/012
2. Wesson, J. (2004). *Tokamaks*: 3rd ed. Oxford: Clarendon Press.
3. Dnestrovskii, Yu. N. & Kostomarov, D. P. (1993). *Matematicheskoe modelirovanie plazmy*: 2nd ed. [Mathematical modeling of plasma]. Moscow, Fismatlit, [in Russian].
4. Zaitsev, F.S. (2014) Mathematical modeling of toroidal plasma evolution. Moscow, MAKS Press.
5. Samoilenko, Yu. I., Gubarev, V. F. & Krivonos, Yu. G. (1988). *Upravlenie bystroprotekayushchimi protsessami v termoyadernykh ustanovkah* [Rapid processes control in the thermonuclear devices]. Kiev, Naukova dumka, [in Russian].
6. Ariola, M. & Pironti, A. (2008). *Magnetic Control of Tokamak Plasmas.* Berlin, Springer.
7. Mitrishkin, Yu.V. (2016). *Upravlenie plazmoi v eksperimentalnykh termoyadernykh ustanovkakh: Adaptivnye avtokolebatelnye i robastnye sistemy upravleniya* [Plasma control in the experimental thermonuclear devices: Adaptive self-oscillating and robust control systems]. Moscow, URSS-KRASAND, [in Russian].
8. Katsuro-Hopkins, O., Sabbagh, S.A. & Bialek, J.M. (2009). Analysis of resistive wall mode LQG control in NSTX with mode rotation. *Proc. Joint 48th IEEE Conference on Decision and Control and 28th Chinese Control Conference*. Shanghai, P.R. China, 309–314.
9. Xu, C. & Schuster, E. (2009). Control of ramp-up current profile dynamics in tokamak plasmas via the minimal-surface theory. *Proc. Joint 48th IEEE Conference on Decision and Control and 28th Chinese Control Conference.* Shanghai, P.R. China, 1367–1372.
10. Mitrishkin, Y.V. & Ivanov, V.A. (2011). Combined nonlinear tokamak plasma current profile control system design with input constraints. *Proc. IFAC World Congress*. Milan, Italy, 3728–3733.
11. Moreau, D., Mazon, D., Adachi, Y., et al. (2009). Identification of the Magneto-Thermal Plasma Response for Plasma State Control in Advanced Tokamaks. *Proc. Joint 48th IEEE Conference on Decision and Control and 28th Chinese Control Conference*. Shanghai, P.R. China, 1379–1386.
12. Felici, F. (2011). Real-time control of tokamak plasmas: from control of physics to physics-based control. *Ph.D Thesis,* École Polytechnique Fédérale de Lausanne (EPFL).
13. Shi, W., Wehner, W., Barton, J., et al. (2012). A Two-time-scale Model-based Combined Magnetic and Kinetic Control System for Advanced Tokamak Scenarios on DIII-D. *Proc. 51st IEEE Conference on Decision and Control*. Maui, Hawaii, USA, 4347–4352.
14. Pironti, A. & Walker, M. (2005). Control of Tokamak Plasmas. Introduction to the special section. *IEEE Control Systems Magazine*, 25(5), 24–29, https://doi.org/10.1109/MCS.2005.1512793

15. Pironti, A. & Walker, M. (2005). Fusion, tokamaks, and Plasma Control. An introduction and tutorial. *IEEE Control Systems Magazine*, 25(5), 30–43, https://doi.org/10.1109/MCS.2005.1512794
16. Balshaw, N. *All-the-World's Tokamaks*. [Online]. Available http://www.tokamak.info
17. Moffat, G. (1980). Vozbuzhdenie magnitnogo polya v provodyashchei srede [Excitation of the magnetic field in the conducting medium]. Moscow, Mir, [in Russian].
18. Federici, G., Biel, W., Gilbert, M.R., et al. (2017) European DEMO design strategy and consequences for materials. *Nuclear Fusion*, 57(9), 26, https://doi.org/10.1088/1741-4326/57/9/092002
19. Kauling, T. (1959). *Magnitnaya gidrodinamika* [Magnetic hydrodynamics]. Moscow, Izd-vo inostrannoi literatury, [in Russian].
20. Walker, M.L., Humphreys, D.A., Leuer, J.A., et al. (2000). *Implementation of model-based multivariable control on DIII–D.* GA–A23468. [Online]. Available https://fusion.gat.com/pubs-ext/SOFT00/A23468.pdf
21. Shi, W., Barton, J., Alsarheed, M. & Schuster, E. (2011). Multivariable Multi-Model-based Magnetic Control System for the Current Ramp-up Phase in the National Spherical Torus Experiment (NSTX). *Proc. of 50th IEEE Conference on Decision and Control and European Control Conference (CDC-ECC)*. Orlando, FL, USA, 26–37.
22. Lister, J.B., Sharma, A., Limebeer, D.J.N., et al. (2002). Plasma equilibrium response modelling and validation on JT-60U. *Nuclear Fusion*, 42(6), 708–724.
23. Hofmann, F., Lister, J.B., Anton, M., et al. (1994). Creation and Control of Variably Shaped Plasmas in TCV. *Plasma Physics and Controlled Fusion*, 36, B277-B287. [Online]. Available https://infoscience.epfl.ch/record/119423/files/0741-3335_31_4_003.pdf
24. Sartori, F., Tommasi & G., Piccolo, F. (2006). The Joint European Torus. Plasma Position and Shape Control in the World's Largest Tokamak. *IEEE Control Syst. Magazine*, 26(2), 64–78, https://doi.org/10.1109/MCS.2006.1615273
25. Mertens, V., Raupp, G., and Treutterer, W. (2003). Chapter 3: Plasma Control in ASDEX Upgrade. *Fusion Science and Technology*, 44(3), 593–604, https://doi.org/10.13182/FST03-A401
26. Yuan, Q.P., Xiao, B.J., Luo, Z.P., et al. (2013). Plasma current, position and shape feedback control on EAST. *Nuclear Fusion*, 53(4), 043009, https://doi.org/10.1088/0029-5515/53/4/043009
27. Lee, G.S., Kwon, M., Doh, C.J., et al. (2001). Design and construction of the KSTAR tokamak. *Nuclear Fusion*, 41(10), 1515–1523, https://doi.org/10.1088/0029-5515/41/10/318
28. Humphreys, D.A, Casper, N.A., Eidietis, N., et al. (2009). Experimental vertical stability studies for ITER performance and design guidance. *Nuclear Fusion*, 49(10), 115003, https://doi.org/10.1088/0029-5515/49/11/115003
29. Gribov, Y., Kavin, A., Lukash, V., et al. (2015). Plasma vertical stabilisation in ITER. *Nuclear* Fusion, 55(7), 073021, https://doi.org/10.1088/0029-5515/55/7/073021
30. Kikuchi, M., JA-EU Satellite Tokamak Working Group & JT-60SA Design Team. (2006). Overview of Modification of JT-60U for the Satellite Tokamak Program as one of the Broader Approach Projects and National Program. *Proc. of 21st IAEA Fusion Energy Conference*, Chengdu, China, FT/2-5.
31. Nerem, A. (1995). DIII-D power supply, design, and development, GA-A-21957, General Atomics. [Online]. Available http://www.iaea.org/inis/collection/NCLCollectionStore/_Public/26/061/26061882.pdf

32. Salewski, M., Geiger, B., Nielsen, S.K., et al. (2013). Combination of fast-ion diagnostics in velocity-space tomographies. *Nuclear Fusion*, 53(6), 063019, https://doi.org/10.1088/0029-5515/53/6/063019
33. Stroth, U., Adamek, J., Aho-Mantila, L., et al. (2013). Overview of ASDEX Upgrade results. *Nuclear Fusion*, 53(10), 104003, https://doi.org/10.1088/0029-5515/53/10/104003
34. Zhang, X., Zhao, Y., Mao, Y., et al. (2011). Current status of ICRF heating experiments on EAST. *Plasma Science and Technology*, 13(2), 172–174, https://doi.org/10.1088/1009-0630/13/2/09
35. Beghi, A. & Cenedesse, A. (2005). Advances in Real-Time Plasma Boundary Reconstruction: from gaps to snakes. *IEEE Control Systems Magazine*, 25(5), 44–64, https://doi.org/10.1109/MCS.2005.1512795
36. Argomedo, F.B., Witrant, E., Prieur, C., et al. (2013). Lyapunov-based distributed control of the safety-factor profile in a tokamak plasma. *Nuclear Fusion*, 53(3), 033005, https://doi.org/10.1088/0029-5515/53/3/033005
37. Khayrutdinov, R.R. & Lukash, V.E. (1993). Studies of plasma equilibrium and transport in a Tokamak fusion device with the inverse-variable technique. *Journal of Computational Physics*, 109(2), 193–201, https://doi.org/10.1006/jcph.1993.1211
38. Jardin, S.C., Pomphrey, N., & Delucia, J. (1986). Dynamic modeling of transport and positional control of tokamaks. *Journal of Computational Physics*, 66(2), 481–507, https://doi.org/10.1016/0021-9991(86)90077-X
39. Genacchi, G., Taroni, A. (1988). JETTO: a free boundary plasma transport code (basic version). Rapporto ENEA RT/TIB 5.
40. Crotinger, J.A., et al. (1997). Lawrence Livermore National lab. Report UCRL-ID-126284, NTIS#PB2005-102154.
41. Rognlien, T.D., Milovich, J.L., Rensink, M.E. & Porter, G.D. (1992). A fully implicit, time dependent 2-D fluid code for modeling tokamak edge plasmas. *Journal of Nuclear Materials*, 196–198, 347–351, https://doi.org/10.1016/S0022-3115(06)80058-9
42. Ivanov, A.A., Galkin, S.A., Drozdov, V.V., et al. (1998). Numerical simulation of free boundary tokamak plasma equilibrium evolution with flux conservation and self-consistent plasma surface current. *40th APS DPP Meeting*. New Orleans, USA. Bulletin of the American Physical Society, 43, 1749.
43. Radford, G.J., Chankin, A.V., Corrigan, G., et al. (1996). The Particle and Heat Drift Fluxes and their Implementation into the EDGE2D Transport Code. *Contributions to Plasma Physics*, 36(2-3), 187–191, https://doi.org/10.1002/ctpp.2150360217
44. Barabaschi, P. (1993). The MAXFEA code, ITER EDA Plasma Control. Technical Meeting, Naka, Japan.
45. Reiter, D. (1992). Progress in two-dimensional plasma edge modeling. *Journal of Nuclear Materials*, 196–198, 80–89, https://doi.org/10.1016/S0022-3115(06)80014-0
46. Takizuka, T. (2011). Development of the PARASOL code and full particle simulation of tokamak Plasma with an Open-Field SOL-Divertor Region Using PARASOL. *Plasma Science and Technology*, 13(3), 316–325, https://doi.org/10.1088/1009-0630/13/3/10
47. Pereverzev, G.V. & Yushmanov, P.N. (2002). ASTRA automated system for transport analysis in a tokamak. *Tech. rep. 5/98.* IPP Report. [Online]. Available http://w3.pppl.gov/~hammett/work/2009/Astra_ocr.pdf
48. Artaud, J.F., Basiuk, V., Imbeaux, F., et al. (2010). The CRONOS suite of codes for integrated tokamak modeling. *Nuclear Fusion*, 50(4), 043001, https://doi.org/10.1088/0029-5515/50/4/043001
49. Hawryluk, R.J. (1981). An empirical approach to tokamak transport. *Physics of Plasmas Close to Thermonuclear Conditions*, 1, 19–46, https://doi.org/10.1016/B978-1-4832-8385-2.50009-1

50. Budny, R.V., Andre, R., Bateman, G., et al. (2008). Predictions of H-mode performance in ITER. *Nuclear Fusion*, 48(7), 075005, https://doi.org/10.1088/0029-5515/48/7/075005
51. Pfeiffer, W.W., Davidson, R H., Miller, R.L., Waltz, R.E. (1980). ONETWO: A Computer Code for Modeling Plasma Transport in Tokamaks. *Technical Report GA-A16178*, General Atomic Company, San Diego, CA, USA.
52. Singer, C.E., Post, D.E., Mikkelsen, D.R., et al. (1988). Baldur: A one-dimensional plasma transport code. *Computer Physics Communications*, 49(2), 275–398, https://doi.org/10.1016/0010-4655(88)90012-4
53. Kim, S.H., Artaud, J.F., Basiuk, V., et al. (2009). Full tokamak discharge simulation of ITER by combining DINA-CH and CRONOS. *Plasma Physics and Controlled Fusion*, 51(10), 105007, https://doi.org/10.1088/0741-3335/51/10/105007
54. Dokuka, V.N., Kdurin, A.V., Mitrishkin, Yu. V., Khayrutdinov, R.R. (2007). Sintez i modelirovanie sistemy magnitnogo upravleniya plazmoi v tokamake-reaktore [Synthesis and modeling of the plasma magnetic control system in a tokamak-reactor]. *Automation and remote control*, 8, 126–145, [in Russian].
55. Walker, M., Humphreys, D. (2006). Valid coordinate systems for linearized plasma shape response models in tokamaks. *Fusion Science and Technology*, 50(4), 473–489, https://doi.org/10.13182/FST06-A1271
56. Lao, L., John, H., Stambaugh, R., et al. (1985). Reconstruction of current profile parameters and plasma shapes in tokamaks. *Nuclear Fusion*, 25(11), 1611–1622, https://doi.org/10.1088/0029-5515/25/11/007
57. Mc Carthy P.J. (1999). Analytical solutions to the Grad–Shafranov equation for tokamak equilibrium with dissimilar source functions. *Physics of Plasmas*, 6(9), 3554, https://doi.org/10.1063/1.873630
58. Korenev, P.S., Mitrishkin, Yu. V., Patrov, M.I. (2016). Rekonstrukciya ravnovesnogo raspredeleniya parametrov plazmy tokamaka po vneshnim magnitnym izmereniyam i postroenie lineinykh plazmennykh modelei [Reconstruction of equilibrium distribution of tokamak plasma parameters by external magnetic measurements and construction of linear plasma models]. *Mechatronics, Automation, Control*, 17(4), 254–265, [in Russian].
59. Forsythe, G., Malcolm, M., Moler, C. (1977). *Computer methods for mathematical computations*. USA, Englewood Cliffs, NJ: Prentice-Hall.
60. Mitrishkin, Yu.V., Korenev, P.S., Prohorov, A.A., Patrov, P.I. (2017). Robust H_∞ switching MIMO control for a plasma time-varying parameter model with a variable structure in a tokamak. *Proc. of IFAC 2017 World Congress*. Toulouse, France, 11883–11888.
61. Sartori, F., Cenedese, A. & Milani, F. (2003). JET real-time object-oriented code for plasma boundary reconstruction. *Fusion Engineering and Design*, 66–68, 735–739, https://doi.org/10.1016/S0920-3796(03)00290-4
62. Braams, B.J., Jilge, W., Lackner. K., et al. (1986). Fast determination of plasma parameters through function parametrization. *Nuclear Fusion*, 26(6), 699–708, https://doi.org/10.1088/0029-5515/26/6/001
63. Zaitsev, F.S., Kostomarov, D.P., Suchkov, T.P., et al. & JET-EFDA Contributors. (2011). Analyses of substantially different plasma current densities and safety factors reconstructed from magnetic diagnostics data. *Nuclear Fusion*, 51(10), 103044, https://doi.org/10.1088/0029-5515/51/10/103044
64. Zaitsev, F.S., Matejcik, S., Murari, A., Suchkov, E.P. & JET-EFDA Contributors. (2012). A new method to identify the equilibria compatible with the measurements using the technique of the ε-nets. *Fusion Science and Technology*, 62(2), 366–373, https://doi.org/10.13182/FST12-476

65. Kostomarov, D.P., Zaitsev, F.S., Suchkov, E.P., Bogdanov P.B. (2014). Reshenie obratnykh zadach metodom epsilon-setei na vysokoproizvoditelnykh EVM [Solution of inverse problems by the method of epsilon networks on high-performance computers]. *Proceedings of the Russian Academy of Sciences*, 455(5), 516–520, [in Russian].
66. Coelho, R., Matejcik, S, McCarthy, P., Suchkov, E.P., Zaitsev, F.S., EU-IM Team & ASDEX Upgrade Team. (2016). Evaluation of epsilon-net calculated equilibrium reconstruction error bars in the European integrated modeling platform. *Fusion Science and Technology*, 69(3), 611–619, https://doi.org/10.13182/FST15-177
67. Zaitsev, F.S., Shishkin, A.G., Lukianitsa, A.A. et al. (2016). Bazovye komponenty apparatno- programmnogo kompleksa modelirovaniya i upravleniya toroidalnoi plazmoi metodom epsilon-setei na geterogennykh mini-superkompyuterakh [Basic components of the hardware-software complex for simulation and control of toroidal plasma by the method of epsilon networks on heterogeneous mini- supercomputers]. *Proc. of NIISI RAS*, 6(1), 36–49, [in Russian].
68. Kolmogorov, A.N., Fomin, S.V. (1976). *Elementy teorii funkcii i funkcionalnogo analiza* [Elements of the theory of functions and functional analysis]. Moscow, Nauka, [in Russian].
69. Zakharov, L.E., Galkin, S.A., Gerasimov, S.N. & JET-EFDA contributors. (2012). Understanding disruptions in tokamaks. *Physics of Plasmas*, 19, 055703, https://doi.org/10.1063/1.4705694
70. Freidberg, J.P. (2014). *Ideal MHD*. Cambridge: Cambridge University Press.
71. Boyd, T.J.M., Sanderson, J.J. (2003). *The physics of plasmas*. Cambridge: Cambridge University Press.
72. Hender, T.C., Wesley, J.C., Bialek, J., et al. (2007). Chapter 3: MHD stability, operational limits and disruptions. *Nuclear Fusion*, 47, S128–S202, https://doi.org/10.1088/0029-5515/47/6/S03
73. *ITER technical basis document* G A0 FDR 1 01-07-13 R1.0. [Online]. Available http://www-pub.iaea.org/MTCD/publications/PDF/ITER-EDA-DS-24.pdf
74. Humphreys, D.A., Ferron, J.R., Hyatt, A.W., et al. (2007). DIII-D integrated plasma control solutions for ITER and next-generation tokamaks. *Proc. of 6th IAEA Technical Meeting on Control, Data Acquisition, and Remote Participation for Fusion Research*, Inuyama, Japan, 193–197.
75. Huang, H, Xu, R., & Gao, G. (2012). Power supply of vertical stability coil in EAST. *AASRI Procedia*, 3, 636–641.
76. Mitrishkin, Yu.V., Kartsev N.M., Zenkov, S.M. (2014). Stabilizaciya neustoychivogo vertikalnogo polozheniya plazmy v tokamake T-15. Part I. [Stabilization of an unstable vertical position of plasma in the T-15 tokamak]. *Automation and remote control*, 2, 129–145, [in Russian].
77. Mitrishkin, Yu.V., Kartsev N.M., Zenkov, S.M. (2014). Stabilizaciya neustoychivogo vertikalnogo polozheniya plazmy v tokamake T-15. Part II. [Stabilization of an unstable vertical position of plasma in the T-15 tokamak]. *Automation and remote control*, 9, 31–44, [in Russian].
78. Kuznetsov, E.A., Yagnov, V.A., Mitrishkin, Y.V., Shcherbitsky, V.N. (2017). Current inverter as actuator for plasma position control systems in tokamaks. *Proc. of the 11th IEEE Intern. Conf. on Application of Information and Communication Technologies (AICT2017)*, Moscow, Russia, 485–489.
79. Mitrishkin, Yu.V., Kartsev, N.M. (2011). Hierarchical plasma shape, position, and current control system for ITER. *Proc. of the 50th IEEE Conf. on Decision and Control*, Orlando, FL, USA, 2620–2625.
80. Mitrishkin, Yu.V., Korenev, P.S., Prohorov, A.A., Patrov, M.I. (2017). Tokamak plasma magnetic control system simulation with reconstruction code in feedback based

on experimental data. *Proc. of 2017 IEEE 56th Annual Conference on Decision and Control*, Melbourne, Australia, 2360–2365.

81. Gusev, V.K., E.A. Azizov, E.A., A.B. Alekseev, A.B., et al. (2013). Globus-M results as the basis for a compact spherical tokamak with enhanced parameters Globus-M2. *Nuclear Fusion*, 53(9), 093013, https://doi.org/10.1088/0029-5515/53/9/093013
82. Mitrishkin, Yu.V., Pavlova, E.A., Kuznetsov, E.A., Gaydamaka, K.I. (2016) Continuous, saturation, and discontinuous tokamak plasma vertical position control systems. *Fusion Engineering and Design*, 108, 35–47, https://doi.org/10.1016/j.fusengdes.2016.04.026
83. Kuznetsov, E.A., Mitrishkin, Yu.V. (2005). *Avtokolebatelnaya sistema stabilizacii neustoichivogo vertikalnogo polozheniya plazmy sfericheskogo tokamaka Globus-M* [Self-oscillating system for stabilizing of an unstable vertical position of the plasma of a spherical tokamak Globus-M]. Moscow, ICS RAS, [in Russian].
84. Gusev, V.K., Golant, V.E., Gusakov, E.Z. et al. (1999). Sfericheskii tokamak Globus-M [Spherical tokamak Globus-M]. *Technical Physics,* 69(9), 58–62, [in Russian].
85. Dyacenko, V.V., Izrak, M.A., Tregubova, E.N. et al. (2003). Postanovka eksperimenta po VCh nagrevu plazmy na sfericheskom tokamake Globus-M [Statement of an experiment on a high-frequency heating of plasma in a spherical Globus-M tokamak]. *Technical Physics,* 73(8), 126–131, [in Russian].
86. Gusev, V.K., Dech, V.K., Esipov, L.A. et al. (2007). Kompleks neitralnoi inzhekcii sfericheskogo tokamaka Globus-M [*Neutral injection complex of the spherical tokamak Globus-M*]. *Technical Physics,* 77(9), 28–43, [in Russian].
87. Sakharov, N.V. (2001). Spherical tokamak Globus-M construction and operation. *Plasma Devices and Operations*, 9(1-2), 25–38, https://doi.org/10.1080/10519990108224485
88. Bulanin, V.V., Gusev, V.K., Chugunov, I.N., et al. (2001). The Globus-M diagnostics design. *Plasma Devices and Operations*, 9(1-2), 129–142, https://doi.org/10.1080/10519990108224492
89. Gusev, V.K., Bakharev, N.N., Belyakov, V.A., et al. (2015). Review of Globus-M spherical tokamak results. *Nuclear Fusion*, 55(10), 104016, https://doi.org/10.1088/0029-5515/55/10/104016
90. Gusev, V.K., Tolstyakov, S.Yu., Varfolomeev, V.I. et al. (2007). Issledovanie elektronnogo komponenta plazmy na sfericheskom tokamake Globus-M v usloviyakh predelnikh plotnostei s pomoshchyu diagnostiki tompsonovskogo rasseyaniya [*Electron component study using thomson scattering in plasma of spherical tokamak Globus-M under the density limits*]. *Problems of atomic science and technology*, 1, 39–56, [in Russian].
91. Gusev, V.K., Bender, V.K., Dech, A.V. et al. (2006). Metody rekonstrukcii ravnovesiya plazmy na sfericheskom tokamake Globus-M [Plasma equilibrium reconstruction methods in the spherical *tokamak Globus-M*]. *Technical Physics,* 76(8), 25–33, [in Russian].
92. Mirnov, S.V. (2016). V.D. Shafranov and Tokamaks. *Journal of Plasma Physics*, 82, 515820102, https://doi.org/10.1017/S0022377816000027

